The Effect of Surface Character on Flows in Microchannels

L.E. Rodd[1], S.T. Huntington[2], K. Lyytikainen[3],
D.V. Boger[1], J.J. Cooper-White[1*]

[1]Particulate Fluids Processing Centre, The Department of Chemical and Biomolecular Engineering, The University of Melbourne, Australia, [2]School of Physics, The University of Melbourne, Australia, and [3]Optical Fibre Technology Centre, The University of Sydney, Australia
[*]Corresponding author: jjcw@unimelb.edu.au

ABSTRACT

A technique for quantifying velocity profiles of fluids flowing in circular microchannels is presented. The primary purpose of this technique is to provide a robust method for quantifying the effect of surface character on the bulk fluid behaviour. A laser-scanning confocal microscope has been used to obtain fluorescent particle images from a 1 micron thick plane along the centreline of hydrophobic and hydrophilic glass capillaries. The velocities of fluorescent particles being carried in pressure-driven laminar flow of a Newtonian fluid have been evaluated at the centreplane of 57.5 micron capillaries using a variation of particle tracking velocimetry (PTV). This work aims to clarify inconsistencies in previously reported [1-12] slip velocities observed in water over hydrophobically modified surfaces at micron and sub-micron lengthscales. A change in the velocity profile is observed for water flowing in hydrophobic capillaries, although the behaviour appears to be a result of an optical distortion at the fluid-wall interface. This may point to previous suggestions of a thin layer of air adsorbing to the surface. Notwithstanding, the results do not confidently suggest evidence of slip of water on hydrophobic surfaces in microchannels.

1. INTRODUCTION

Effective design of microdevices for biofluid analysis relies on a fundamental understanding of the properties of the fluid being transported, its interactions with the surface, and the propagation of these interactions within the bulk flow. Such fluid-surface interactions are dependent on both the fluid properties and the surface character, which can be defined according to its roughness, charge density, hydrophobicity and surface heterogeneity. In traditional macro-scale fluid dynamics, fluid-surface interactions are simplified by a general boundary condition (eg. slip or no-slip). However, as the size of the channel reduces, the length-scales of surface features (eg. surface roughness and surface heterogeneity) become more comparable to the lengthscale of the microchannel itself. Following from this, one may expect to see fluid behaviour that is dependent on the surface properties, even for Newtonian pressure driven flows. One such example of this is the slip of polar Newtonian fluids on hydrophobic surfaces. The majority of measurements of slip on hydrophobic surfaces have been made through bulk pressure drop and flowrate measurements. One of the earlier examples of this is the work of Schnell [1] in 1956, who measured a 0-5% increase in flowrate inside 15 mm diameter hydrophobic capillaries, when compared with hydrophilic capillaries, for the same pressure drop. Watanabe et al. [2] performed similar experiments at the same lengthscale (16 mm diameter capillaries) and observed similar behaviour, such that a 14% drag reduction was observed in the laminar flow regime. The first slip flow experiments in micron-sized capillaries were performed by Churaev et al. [3] in 1983. They performed similar experiments in 1.7-14 micron diameter channels, and quantified a slip length of ~30nm by fitting pressure drop and flowrate data to the slip-corrected Hagen-Poiseuille equation, whose boundary conditions concur with Navier's Hypothesis for fluid slip (Equation 1). Choi et. al [4] calculated the same slip length in hydrophobic 1-2 micron deep rectangular microchannels. They also established a linear dependence of slip length on shear rate, such that a slip length of 30 nm was found at a wall shear rate of 50 000s^{-1} (wall shear stress = 50 Pa).

Measurements of slip on hydrophobic surfaces have also been obtained through Surface Force Apparatus (SFA) experiments [5-8]. This involves measuring the hydrodynamic drainage forces associated with liquid draining from two approaching surfaces as a function of separation distance. Zhu and Granick [5-6] systematically varied surface

BioMEMS and Nanotechnology, edited by Dan V. Nicolau, Uwe R. Muller, John M. Dell, Proceedings of SPIE Vol. 5275 (SPIE, Bellingham, WA, 2004)
0277-786X/04/$15 · doi: 10.1117/12.530223

roughness (0.2-1.2nm) and surface wettability (12-121^o) to show that both roughness and surface hydrophobicity increased the deviations of the hydrodynamic force from that predicted according to the no-slip boundary condition. However, the surface hydrophobicity was only found to have an effect up to a roughness of 2nm, beyond which roughness dominated. Slip lengths of up to 2.5 microns were inferred from hydrodynamic force measurements for separation distances of 20-300 nanometers. These values for slip length are quite high compared to those measured by Baudry et al. [6], who found slip lengths of around 40 nm, based on their SFA measurements using glycerol. Measurements in shear cells have also been used to indirectly determine a slip length via Total Internal Refelction-Fluorescence Recovery After Photobleaching (TIR-FRAP). Pit et al. [9] measured a slip length of 300nm in a 190 micron gap shear cell containing hexadecane on a partly wetting surface. Their TIR-FRAP technique allowed them to probe distances of 100nm from the wall.

Tretheway and Meinhart [10] were the first to directly measure a slip velocity through micro-Particle Image Velocimetry (μ-PIV) measurements. They observed slip lengths on the same order of magnitude as those by Zhu and Granick [5], by directly measuring fluid velocities to within 450 nm of the wall. They measured a slip length of 1 micron in water flows over hydrophobic microchannels with 30 x 300 micron cross-sections. There is however, some ambiguity associated with the wall position, which is estimated according to the onset of erroneous velocity vectors calculated through a PIV cross-correlation algorithm. Their slip length of 1 micron was found at a wall shear rate of 880s^{-1} (wall shear stress = 0.9 Pa), however the dependence of slip length on shear rate could not be determined due to the limited number of experiments. Watanabe et al. [2] also measured a slip velocity directly through velocity measurements using hot wire anemometry, although these experiments were conducted in 16 mm capillaries.

The majority of experimental evidence of slip, which has primarily been inferred through bulk measurements, suggests slip lengths of the order of 10's – 100's nanometers. This order of magnitude agrees with the molecular dynamics simulations by Barrat and Bocquet [11], who calculate a slip length on the order of 30 molecular diameters for contact angles of 140^o. However, the inconsistency in slip lengths measured both indirectly and directly, may be explained by the work of Ruckenstein and Rajora [12]. They conjectured that slip on solid surfaces occurs over a gap, rather than on the surface itself. This conclusion followed their prediction of the surface diffusion coefficient and comparison with values calculated from experiment. The over-prediction of the surface diffusion coefficient through previous experimental results suggested the existence of a finite gap between unlike solids and liquids. It was suggested that the thickness of this gap may be dependent on the likelihood of soluble gases desorbing from solution.

The work presented here quantifies the velocity profiles of water flowing in 57 micron diameter circular microchannels with both hydrophilic and hydrophobic surfaces. A variation of a particle tracking velocimetry (PTV) technique is implemented using images obtained from a laser-scanning confocal microscope. Tracer particle velocities are measured to within 1 micron of the wall, for a range of flowrates, corresponding to wall shear rates between 300-1640s^{-1} and Reynolds numbers between 0.13 - 0.70. Experiments were done using both water (wall shear stress = 0.2 - 1.7 Pa) and for a mixture of ethylene glycol and hexanol (wall shear stress = 3.0 – 12.2 Pa). The ethylene glycol mixture was used for the purpose of eliminating refractive effects by index matching with the glass capillary.

2. THEORY

In classical macro-scale fluid dynamics, the velocity profile for low Reynolds number flows, inside a circular cross-sectioned channel with a no-slip boundary condition is given by the Hagen-Poiseuille Equation,

$$v(r) = \frac{2Q}{\pi R^2}\left(1 - \left(\frac{r}{R}\right)^2\right) \quad , \tag{1}$$

where r is the radial distance from the centreline, R is the capillary radius and Q is the volumetric flowrate. In the presence of slip, the Navier slip hypothesis defines a slip velocity according to

$$v_s = L_s \left.\frac{\partial v}{\partial r}\right|_{r=R} \quad , \tag{2}$$

where $\partial v / \partial r\big|_{r=R}$ is the shear rate at the wall and L_s is the slip length, which is defined as the theoretical distance below the wall to where the velocity extrapolates to zero. Under such slip conditions, the velocity profile becomes

$$v(r) = \frac{2Q}{\pi R^2}\left(1 - \left(\frac{r}{R}\right)^2 + \frac{2L_s}{R}\right)\left(1 + \frac{4L_s}{R}\right)^{-1} \quad , \tag{3}$$

The primary difficulty with imaging flows in circular microchannels is an apparent shift in the velocity profile due to a mismatch in refractive indices ($n_1 \neq n_2$) at the water/glass interface. This becomes increasingly important in microchannels (compared with their macroscale counterpart), due to the high curvature of the interface. Particle images appear to be located closer to the centreline (for $n_2 > n_1$), as illustrated in Figure 1. Outside curvature effects can be eliminated by immersing the microchannel in an index matching fluid, such as glycerol ($n_1 = n_2$).

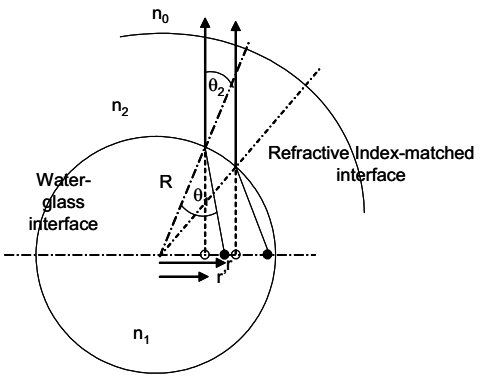

Figure 1. Microchannel cross-section; shift in particle image due to refraction at the water-glass interface (particle image location, r' (o), real particle location, r (•), θ_1 = angle of incidence, θ_2 = angle of refraction, n_1, n_2 and n_o are the refractive indices of the bulk fluid, channel material and outside fluid, respectively.

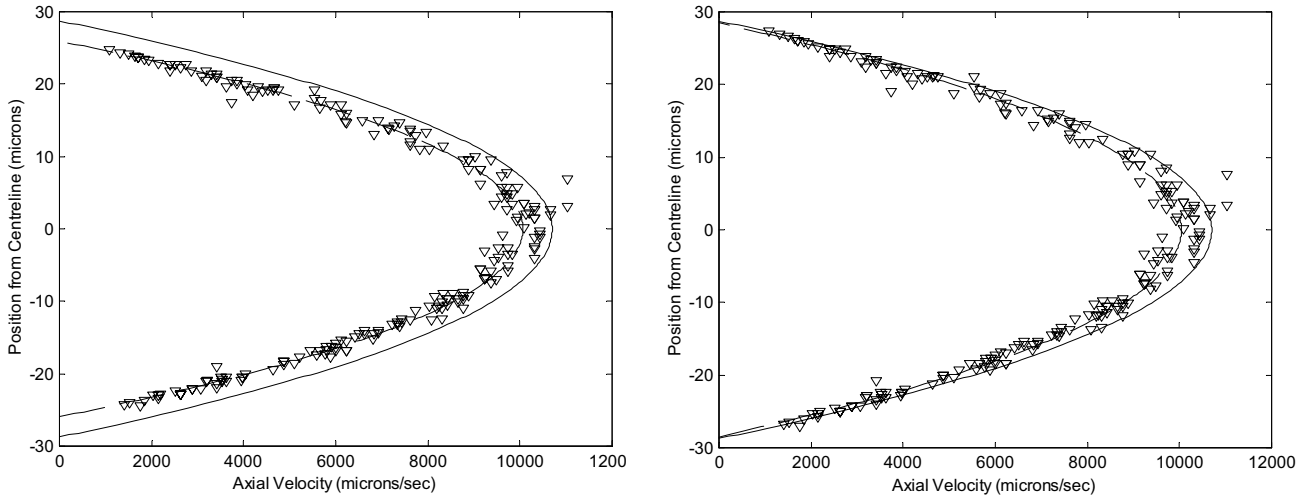

(a) (b)

Figure 2. Distortion in velocity profile due to refraction at the water-glass interface; (a) uncorrected profile (b) corrected profile using Equation 4; ∇ is the measured velocity (raw data (a) and corrected data (b)) , --- is the line of best fit to the data, and — is the prediction based on Equation 1.

The effect illustrated in Figure 1 becomes more pronounced for locations nearest the wall of the capillary where the angle of incidence increases. Figure 2 illustrates the effect of this apparent shift in particle location on the measured velocity profile. An adjustment to measured particle locations can be made according to equation 4,

$$r = r'\left(\frac{\tan\left(\sin^{-1}\left(\frac{n_2 r'}{n_1 R}\right) - \sin^{-1}\left(\frac{r'}{R}\right)\right)}{\tan\left(\sin^{-1}\left(\frac{r'}{R}\right)\right)} + 1\right) \quad , \tag{4}$$

where n_1 and n_2 are the refractive indices of the bulk fluid and channel material, respectively, r is the adjusted particle position and r' is the 'apparent' particle image position. The need for this correction is eliminated by matching the refractive index of the transported fluid with that of the glass, such that $n_1=n_o$.

3. EXPERIMENTAL

57 micron diameter microchannels were fabricated from drawn optical fibres. The optical fibres are optically smooth and are expected to have a roughness in the order of nanometers, however its roughness has not been measured due to the difficulty of probing the inside surface. Their surfaces were hydrophobized using a silanization treatment. Water seeded with 210 nm fluorescent latex particles (Interfacial Dynamics Corporation) was delivered at a range of flowrates between 20 and 110 μLhr^{-1} using a Harvard PHD2000 syringe pump. A second fluid, index matching with the channel material ($n_1=n_2$), was also used as the carrier fluid to provide a refraction-free experiment that could be used to verify the correctness of the velocity measurements. This index matching solution was a 2:1 mixture of ethylene glycol and hexanol, which satisfied the requirement for neutral buoyancy and chemical compatibility with the suspended particles.

A 10μL syringe was used to deliver the bulk fluid to avoid pulsated flow associated with the stepper motor of the syringe pump, which is typically observed at very small volumetric flowrates. Excitation and detection of 210 nm fluorescent particles was achieved using a multi-line Argon ion laser at 488nm and an Olympus FluoView FV500 Laser-scanning Confocal Microscope. The confocal microscope uses a laser scanning system and photomultiplier tube, whereby an image is formed only through a reconstruction of pixels generated individually via point-by-point detection. The laser-scanning confocal microscope was operated in a fast scanning mode, achieving a scanning rate of 0.17 ms^{-1} in the object plane. Particle velocities were measured to within 1 micron of the wall and over the entire width of the channel.

3.1 Surface Modification

Hydrophilic surfaces were prepared using a solution of aqueous ammonia (30% wt.), hydrogen peroxide (28% wt.) and water at a volumetric ratio of 1:1:5. A solution containing only the aqueous ammonia and water components was heated to 80^{o}C, at which point hydrogen peroxide was added. Exposure of the surfaces to this solution was maintained for 20 minutes after the addition of hydrogen peroxide. Surfaces were rinsed multiple times with water and then dried. This step was also used in the preparation of hydrophobic surfaces, which was achieved using a 5mmol solution of octadecyltrichlorosilane (OTS) in a hydrocarbon solvent (mineral turpentine). Exposure to this solution was maintained under static conditions for 1.5 hours at 12^{o}C.

Static contact angle measurements for water on a flat glass surface gave values of 118^o and 10^o for the hydrophobic and hydrophilic surfaces, respectively. Images of an air-water interface inside the channels were also used as a qualitative measure of the degree of hydrophobicity achieved using these treatment methods. Figure 3 illustrates the degree of hydrophobicity in the hydrophilic (a) and hydrophobic (b) channels, where the phase on the left of the interface is water and on the right side of the interface is air. The interface shown in Figure 3(b) is in inverted, such that the crown of the interface is pointing to the right.

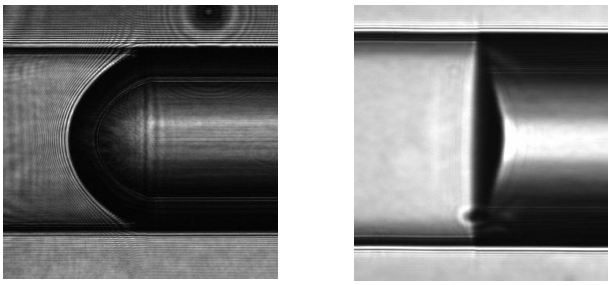

(a) (b)

Figure 3. Air/water interface inside circular microchannels with an a) hydrophilic and b) hydrophobic surface

The contact angles for ethylene glycol/hexanol on the hydrophobic surface were substantially lower (~45^{o}), compared with that of water (~120^{o}). These measurements were steady in time, suggesting that the ethylene glycol/hexanol mixture did not absorb into the OTS layer. Due to the low contact angle, the ethylene glycol/hexanol mixture was not expected to exhibit a slip velocity over the hydrophobic surface, but rather provide a partly wetting system that allows velocity measurements that are unaffected by optical distortion.

3.2 Confocal Microscopy and Particle Images

Figure 4 is an example of an image of moving particles taken using a laser-scanning confocal microscope. The scanning nature of the microscope results in images that are acquired over time. The time taken to scan the entire frame is dependent on the number of lines being scanned and the scanning speed of the laser. Each frame therefore consists of a time-series of images for each particle, which effectively appear as streaks. The images within each of the boxes highlighted in Figure 4 are a series of images for a single particle that has displaced over a known time. The time for each displacement can be calculated from the scanning speed of the laser, the position of the particle, the displacement in the axial direction, and the number of lines scanned during this period. It is then possible to calculate a velocity for each particle.

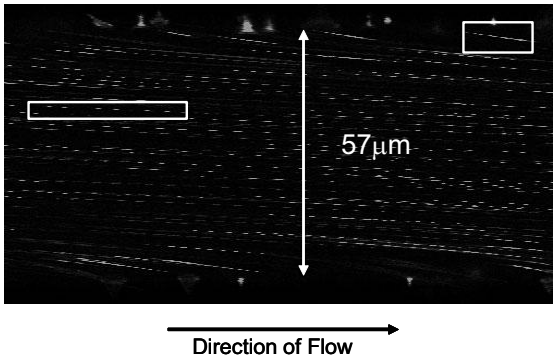

Figure 4. A single frame acquired using a laser-scanning confocal microscope and photomultiplier tube (PMT); 210nm fluorescent particles flowing inside a 57 micron circular microchannel.

For flows that are steady in time, multiple frames can be used to extract a large number of particle velocities as a function of radial position. In all experiments, velocity data is acquired over the entire width of the channel, which means there is no ambiguity regarding the location of the wall. The maximum of a least-squares fit to the data is aligned with the centre axis of the channel in order to correctly position each of the profiles with reference to the geometry. The correctness of this alignment procedure is verified in the velocity profiles for the hydrophilic case, where a no-slip boundary condition is expected.

4. RESULTS AND DISCUSSION

The velocity profiles for water over the hydrophilic channel are presented in Figure 5, for flowrates between 20 and 110 μLhr^{-1}. The corresponding shear rates range between 300s^{-1} and 1640s^{-1} and Reynolds numbers between 0.13 - 0.7. The measured velocities have been compared to those predicted by Equation 1. The dotted lines in Figures 5 and 6 are the least-squares fit to the data. The measured velocities agree reasonably well with the predicted velocity profiles. In the region nearest the wall, the line of best fit to the data suggests that the velocity profile extrapolates to zero at the wall. Flowrates calculated by integrating beneath the velocity profiles were within ±9% of the set flowrate. There is very little scatter in the data for velocities below 0.015 m.s^{-1}, though this is seen to increase substantially for higher velocities. It is suspected that this scatter could be a result of optical distortions experienced in the axial direction, which have not been considered.

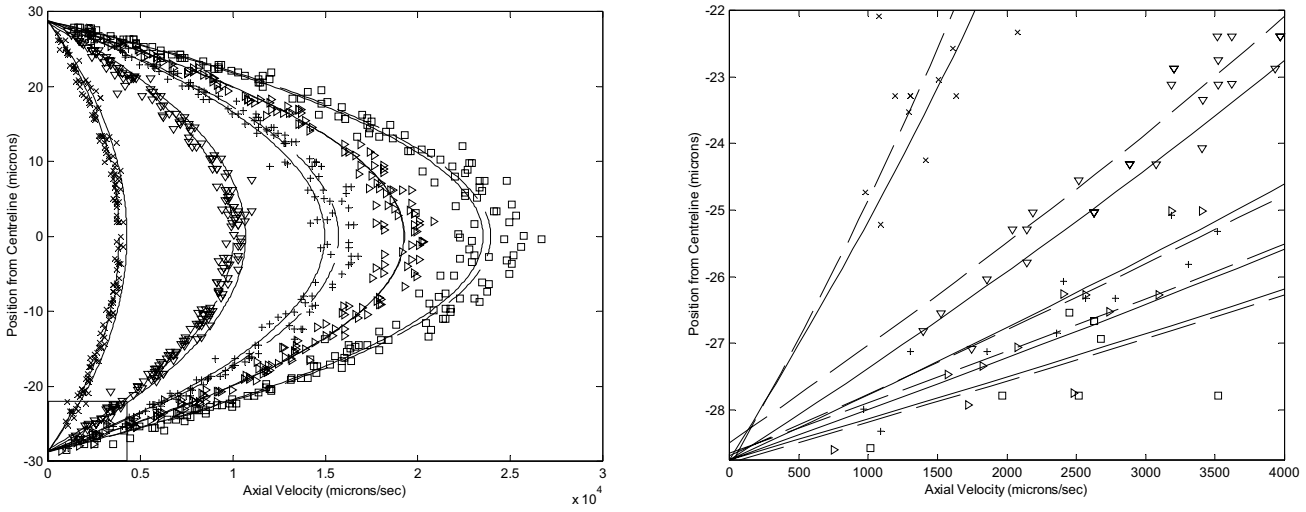

(a) (b)

Figure 5. Measured velocity profiles of water flowing in a 57.5 micron diameter hydrophilic channel for flowrates, × 20, ▽50, + 70, ▷90, □ 110μLhr^{-1}; (a) full field profile (b) profile within 8 microns of the wall, where — is the prediction based on Equation 1, and – – is the least squares fit to the data.

Figure 6 illustrates the velocity profiles for water flowing through the hydrophobically modified microchannels. These experiments were operated under the same flowrate conditions as those in the hydrophilic case. The corresponding range of shear rates are comparable to and exceed that of Tretheway and Meinhart [10], who reported slip at a shear rate of 800s^{-1}, for the same fluid-surface system in a rectangular channel.

A velocity profile associated with a slip boundary condition would appear to have a higher velocity for the same radial position, with a lower maximum velocity at the centreline, such that the total volumetric flowrate is conserved. However, the results in Figure 6 do not suggest any form of slip at the wall. On the other hand, the velocity profiles appear to be distorted, such that a lower velocity is observed for the same radial position. At a position of 5 microns from the wall, the measured velocity is 70-80% of the velocity predicted according to Equation 1. This is consistent for all flowrates, whilst the degree of 'distortion' appears to magnify in regions nearest the wall.

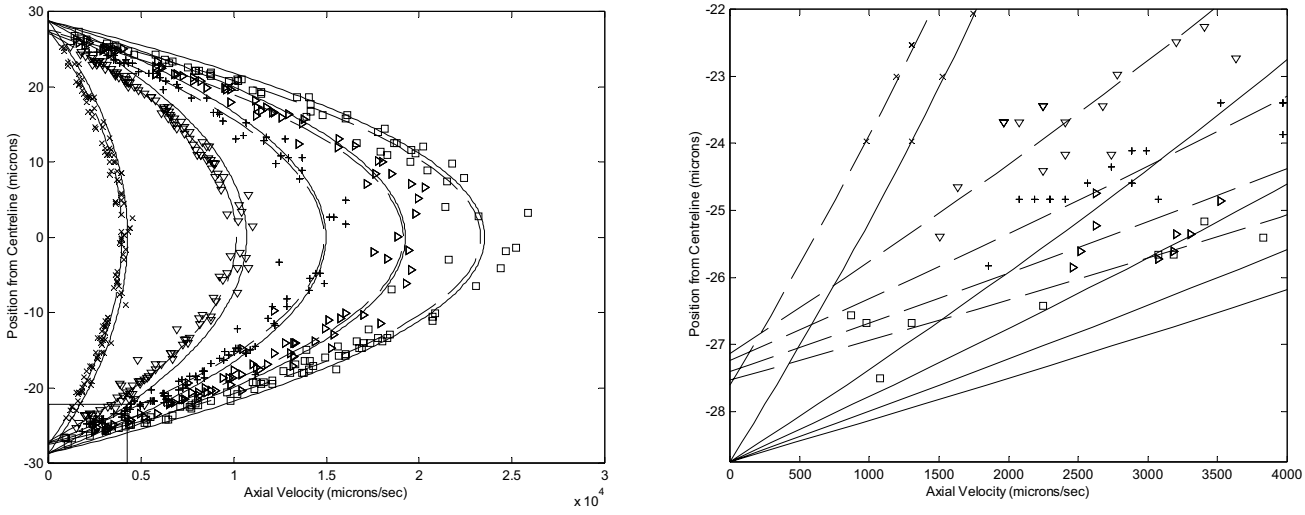

(a) (b)

Figure 6. Measured velocity profiles of water flowing in a 57.5 micron diameter hydrophobic channel for flowrates, × 20, ▽ 50, + 70, ▷ 90, □ 110μLhr^{-1}; (a) full field profile (b) profile within 8 microns of the wall, where — is the prediction based on Equation 1, and – – is the least squares fit to the data.

One possible explanation for this is the existence of a thick hydrophobic layer, causing an effective reduction in diameter. Two pieces of experimental evidence discard this hypothesis. Firstly, a reduction in the channel diameter would result in a higher velocity toward the centreline, for the same volumetric flowrate. Figure 6 illustrates that the maximum velocity at the centreline is not significantly different, compared with the hydrophilic case. Calculating the flowrate by integrating the least squares fit of the velocity profile gives an under-prediction of the set volumetric flowrate. All flowrates were under-predicted by between 9 and 17% of the set flowrate.

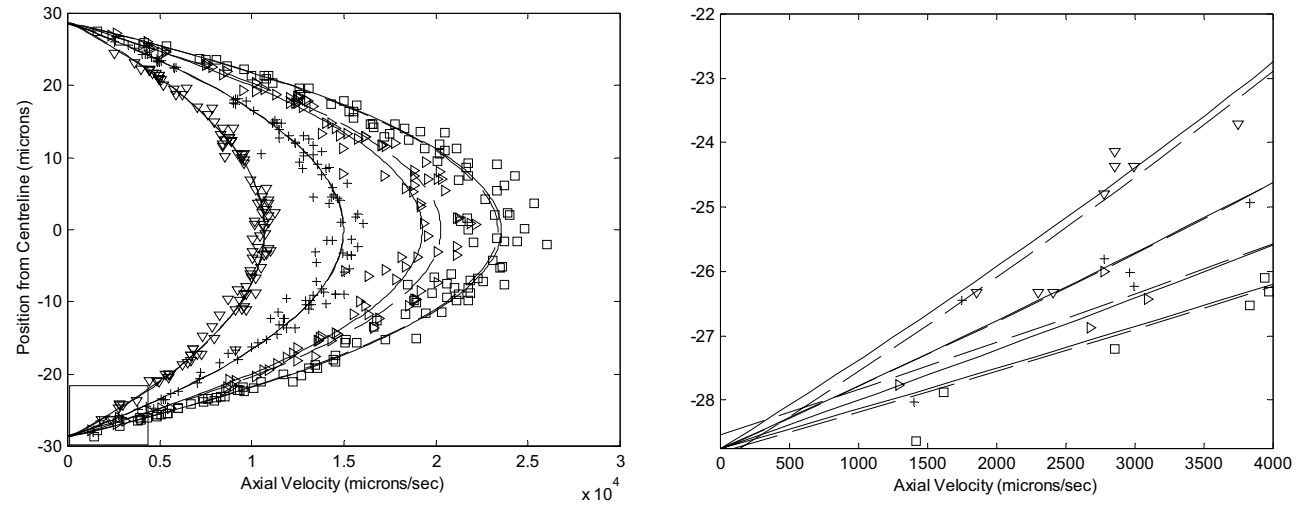

(a) (b)

Figure 7. Measured velocity profiles of ethylene glycol/hexanol flowing in a 57.5 micron diameter hydrophobic channel for flowrates, × 20, ▽ 50, + 70, ▷ 90, □ 110μLhr^{-1}; (a) full field profile (b) profile within 8 microns of the wall, where — is the prediction based on Equation 1, and – – is the least squares fit to the data.

As an additional test, the velocity profiles of ethylene glycol/hexanol over the hydrophobic surface were measured in order to determine any reduction in channel diameter. By using ethylene glycol/hexanol as the bulk fluid, a reduction in channel diameter would be evident in the velocity profile, due to the index matching nature of this system. Figure 7 illustrates the velocity profiles measured for ethylene glycol/hexanol over the hydrophobically modified channel at flowrates between 50 and 110 μLhr^{-1}. The measured profiles agree with the Hagen-Poiseuille predictions for the 57.5 micron diameter channel, suggesting that the channel diameter is unchanged. These secondary experiments were also intended to test the existence of an additional refractive component associated with the hydrophobic layer itself, which should be detectable to some degree, regardless of the fluid being tested. The absence of any velocity profile 'distortion' in Figure 7, suggests this is not the case.

A further possibility is the presence of a thin layer of air, specific to the water-OTS surface system. Previous authors [10] suggest the possibility of undissolved gases from solution adsorbing to the hydrophobic surface. These circumstances would be expected to increase the likelihood of slip, though this is not explicitly obvious from Figure 6. The solutions used in these experiments, have not been degassed, hence the presence of air bubbles on the surface is plausible. In the case of an OTS/air layer, there may exist a coupling of two effects; a slip effect, and an additional optical distortion due to refraction at this new interface. Regardless of this, there is still no obvious change in centreline velocity, which would be expected in the presence of slip. Although the thickness of this air layer is unlikely to be large enough to cause an effective reduction in diameter, it is possible that this is great enough to result in an additional refractive component. This is particularly the case near the wall, where the angle of incidence is higher and the depth of air that is penetrated by a single light ray is also greater. Decoupling slip and this additional refractive component is not possible with these experiments, however the consistency in the centreline velocities between the hydrophobic and hydrophilic experiments strongly suggests that any degree of slip that may be occurring is too small to be detected by particle velocimetry techniques.

5. CONCLUSIONS

The velocity profiles for water flowing over a hydrophilic surface in a 57.5 micron cylindrical microchannel agree with the predictions of the Hagen-Poiseuille Equation for flowrates between 20 and 110 μLhr^{-1}. The profiles for an ethylene glycol/hexanol mixture agree with these predictions for both the hydrophobic and hydrophilic surfaces as expected, since these are moderately and completely wetting systems, respectively. However, a change in the velocity profile is seen for water flowing over the hydrophobically modified surface. The profiles suggest a reduction in velocity for the same radial position, in regions nearest the wall, which is contrary to that expected in slip flows. The measured velocity is consistently 70-80% of the expected velocity for a position at 5 microns from the wall**.** The possibility of a thick hydrophobic layer causing an effective reduction in diameter, and hence a change in profile was considered. This hypothesis was dismissed since the same behaviour is not observed using a partly-wetting, index matching fluid as the bulk. It is suspected that the distorted profiles observed in the water-hydrophobic surface system, is partly the result of an optical distortion due the presence of a thin layer of air at the surface-fluid interface, which is only formed when using water as the bulk fluid. Any accompanying slip effect due to the presence of this air layer could not be decoupled from the effects associated with refraction at the OTS-air/liquid interface. The consistency in the centreline velocities between the hydrophilic and hydrophobic cases, suggest that any existing slip is too small to be detected using particle tracking velocimetry.

ACKNOWLEDGMENTS

The authors would like to acknowledge the Particulate Fluids Processing Centre for infrastructure support and the Smorgon family for their support through the Anne and Eric Smorgon Memorial Award.

REFERENCES

1. Schnell, Erhard, *Slippage of Water over Nonwettable Surfaces*, Journal of Applied Physics, 1956. **27**(10): 1149-1152.

2. Watanabe, Keizo, Yanuar and Hiroshi Udagawa, *Drag reduction of Newtoniana fluid ina circular pipe with a highly water-repellant wall*, Journal of Fluid Mechanics, 1999. **381**: 225-238.

3. Churaev, N.V., V.D. Sobolev and A.N. Somov, *Slippage of Liquids over Lyophobic Solid Surfaces*, Journal of Colloid and Interface Science, 1984. **97**(2): 574-581.

4. Choi, Chang-Hwang, K. Johan A. Westin, and Kenneth S. Breuer, *Apparent slip flows in hydrophilic and hydrophobic microchannels*, Physics of Fluids, 2003. **15**(10): 2897-2902.

5. Zhu, Yingxi and Steve Granick, *Rate-Dependent Slip of Newtonian Liquid at Smooth Surfaces*, Physical Review Letters, 2001. 87(9): 096105-1 – 096105-4.

6. Zhu, Yingxi and Steve Granick, *Limits of the Hydrodynamic No-Slip Boundary Condition.* Physical Review Letters, 2002. **88(10)**: 106102-1 – 106102-4.

7. Baudry, J., E. Charlaix, A. Tonck, and D. Mazuyer, *Experimental Evidence for a Large Slip Effect at a Nonwetting Fluid-Solid Interface*, Langmuir, 2001. **17**: 5232-5236.

8. Craig, Vincent S.J., Chiara Neto, and David R.M. Williams, *Shear-Dependent Boundary Slip in an Aqueous Newtonian Liquid*, Physical Review Letters, 2001. **87**(5): 054504-1 – 054504-4.

9. Pit, R., H. Hervet, and L. Leger, *Direct experimental evidence of slip in hexadecane-solid interface,* Physical Review Letters, 2000. **85**(5): 980-983.

10. Tretheway, Derek C. and Carl D. Meinhart, *Apparent fluid slip at hydrophobic microchannel walls*, Physics of Fluids, 2002. **14**(3): L9-L12.

11. Barrat, Jean-Louis, Lydéric Bocquet, *Large Slip Effect at a Nonwetting Fluid-Solid Interface,* Physical Review Letters, 1999. **82**: 4671-4674.

12. Ruckenstein, E. and P. Rajora, *On the No-Slip Condition of Hydrodynamics*, Journal of Colloid and Interface Science, 1983. **96**(2): 488-491.